


High Expression of *THBS1* Leads to a Poor Prognosis in Papillary Thyroid Cancer and Suppresses the Anti-Tumor Immune Microenvironment

Technology in Cancer Research & Treatment
 Volume 21: 1–17
 © The Author(s) 2022
 Article reuse guidelines:
sagepub.com/journals-permissions
 DOI: 10.1177/15330338221085360
journals.sagepub.com/home/tct


Anqi Jin, MD*, Jin Zhou, MD*, Pengcheng Yu, MD, Shichong Zhou, MD, and Cai Chang, MD 

Abstract

Objectives: To study the role of thrombospondin-1 (THBS1) in papillary thyroid cancer (PTC) prognosis and the immune microenvironment. **Methods:** A retrospective cohort study was designed, and data from The Cancer Genome Atlas database and PTC tissues from Fudan University Shanghai Cancer Center were used. Weighted gene co-expression network analysis was performed to build a *THBS1*-immune-related gene prognostic index (T-I index). **Results:** High *THBS1* expression was correlated with advanced TNM stage, higher recurrence risk, and shorter progression-free interval. High *THBS1* expression correlated with MAPK and PDI pathways indicating a tumor promoting and immunity-inhibiting tendency. The T-I index showed a powerful capacity to predict progression-free survival and immunotherapy benefit. **Conclusion:** High expression of *THBS1* leads to a poor prognosis in PTCs and suppresses the anti-tumor immune microenvironment.

Keywords

papillary thyroid cancer, THBS1, tumor immunity, prognostic signature, immune checkpoint inhibitor therapy

Abbreviations

ATA, American thyroid association; BP, biological progress; CC, cellular component; C-PTC, classical PTC; ESTIMATE, Estimation of STromal and Immune cells in Malignant Tumor tissues using Expression data; ETE, extrathyroidal extension; FTC, follicular thyroid carcinoma; FUSCC, Fudan University Shanghai Cancer Center; FV-PTC, follicular variant PTC; GSEA, gene set enrichment analysis; GO, gene ontology; ICI, immune checkpoint inhibitor; IF, immunofluorescence; IHC, immunohistochemical; KEGG, Kyoto Encyclopedia of Genes and Genomes; MF, molecular function; MM, module membership; PFI, progress free interval; PFS, progress free survival; PTC, papillary thyroid carcinoma; ROC, receiver operator characteristic curve; T-I, THBS1-immune; TCV-PTC, tall cell variant PTC; TFH, follicular helper t cell; THBS1, thrombospondin-1; TIDE, Tumor Immune Dysfunction and Exclusion; TIMER, Tumor Immune Estimation Resource; TME, tumor microenvironment; TPM, transcript per million; WGCNA, weighted gene co-expression network analysis

Received: November 10, 2021; Revised: February 11, 2022; Accepted: February 17, 2022.

Introduction

Thyroid cancer is the most common malignant tumor of the endocrine system,¹ and the incidence of thyroid cancer, especially papillary cancer, has been increasing.² Most papillary thyroid cancers (PTCs) can be surgically removed and show a good overall prognosis and low fatality rate.³ However, a considerable number of patients show cervical lymph node metastasis and need to undergo cervical lymph node dissection

Fudan University Shanghai Cancer Center, Shanghai, China

*These authors have contributed equally to this work and share first authorship.

Corresponding Author:

Cai Chang, Department of Ultrasound, Fudan University Shanghai Cancer Center, No. 270 Dong'an Road, Shanghai 200032, China.
 Email: caichang_fuscc@hotmail.com



Creative Commons Non Commercial CC BY-NC: This article is distributed under the terms of the Creative Commons Attribution-NonCommercial 4.0 License (<https://creativecommons.org/licenses/by-nc/4.0/>) which permits non-commercial use, reproduction and distribution of the work without further permission provided the original work is attributed as specified on the SAGE and Open Access page (<https://us.sagepub.com/en-us/nam/open-access-at-sage>).

surgery,⁴ which seriously impacts the postoperative quality of life. Advanced PTCs, such as tumors with a large cervical mass and extensive extrathyroidal invasion of tumors, are more difficult to operate on, and postoperative adverse reactions can occur, such as cervical recurrent laryngeal nerve injury.⁵ Therefore, the identification of molecular markers of advanced PTCs and the corresponding therapeutic targets is critical improving patient treatment.

The tumor microenvironment (TME) plays an important role in all stages of tumor development and contains multiple components, including tumor cells, tumor stromal cells, and immune cells. Immune cells within the TME have key functions in tumorigenesis, with both tumor-promoting and tumor-suppressive roles.⁶ Recent years have seen the development of immunotherapy as cancer treatments that function by activating innate immunity or blocking immune checkpoints. Although a large number of studies have shown that immunotherapy has beneficial effect on a variety of tumors,^{7,8} the research on immunotherapy for thyroid cancer, especially for advanced PTCs, is limited.^{9,10} Given the limited response to immunotherapy, it is important to identify immunotherapy-related targets and patients who can benefit from immunotherapy.

Thrombospondin-1 (THBS1) is a member of the thrombospondin protein family.¹¹ It is a large matricellular glycoprotein, with various protein-binding domains. THBS1 has multiple biological functions, such as in wound repair and tissue generation. Recent studies have shown that THBS1 is also involved in cancer development.¹² THBS1 plays 2 major roles in tumors. THBS1 inhibits neovascularization in tumors^{13,14} but also promotes tumor invasion and metastasis. This process is regulated by different pathways in different tumors.¹⁵ For example, in breast tumors, THBS1 regulates tumor cell adhesion and invasion by upregulating MMP-9¹⁶ or TGF- β ¹⁷ or activating the urokinase plasminogen system,¹⁸ thus promoting tumor invasion and metastasis, as observed in breast cancer¹⁹ and thyroid cancer.²⁰ In our imaging histology research on cervical lymph node metastasis ultrasound images of thyroid cancer, high THBS1 expression negatively correlated with lymph node metastasis,²¹ which is inconsistent with the previous study.²² However, our imaging histology research mainly focused on ultrasound images of PTCs and did not explore the function of *THBS1* in tumors. We also noted a correlation between the gene module with *THBS1* as the hub gene and tumor immunity. In view of studies showing that *THBS1* has a role in suppressing the antitumor immune microenvironment in gastric cancer,²³ we believe that the role of *THBS1* in PTC and the role it plays in the tumor immune microenvironment is worthy of investigation.

In this study, we performed a preliminary analysis on the expression level and possible role of THBS1 in PTCs using data from a public database and clinical specimens that were retrospectively collected. We further designed a *THBS1*-immune-related gene prognostic index (T-I index) based on *THBS1* and immune-related genes and studied its efficacy as a predictor of thyroid cancer prognosis and immunotherapy response.

Methods and Materials

Patient Data Acquisition

The reporting of this study conforms to STROBE guidelines.²⁴ Thyroid carcinoma patient datasets, with gene expression profiles and clinical information, were downloaded from the publicly available The Cancer Genome Atlas TCGA-THCA project. This project included 507 cases with 510 tumor samples and 58 paired normal samples. We applied the following exclusion criteria in the study analyses: (1) samples with incomplete clinical data were excluded from the subgroup comparison, and (2) in certain subgroup analyses, normal tissue samples were excluded. After data sorting, RNA sequencing data of 503 tumor samples and 58 paired normal samples were converted to RNA seq data in transcript per million (TPM) format.

For the validation cohort, 53 patients with paired PTC and normal tissues were retrospectively enrolled from Fudan University Shanghai Cancer Center (FUSCC). We obtained frozen tumor tissues and the related pathological data from the Department of Biobank and Pathology at the FUSCC. The inclusion criteria were as follows: (1) tissue specimens were completely preserved in liquid nitrogen or at -80°C , with sufficient sample size for RNA extraction and sectioning, (2) one or more follow-up visits were recorded, and (3) the medical history and examination data were complete.

All research protocols were approved by the ethical committee of FUSCC (approval 2101-ZZK-41) and all enrolled patients signed informed consent forms.

Survival and Clinical Correlation Analysis

To maintain consistency of grouping criteria within the same study, TNM stage and extrathyroidal extension (ETE) were defined according to the 7th edition of American Joint Committee on Cancer guidelines. In this research, ETE includes both cases of tumor breaking through the perithelium and invasion by extra-thyroidal peripheral adipose tissue; this type of tumor is classified as T3. Since thyroid carcinoma patients show a good overall survival, we selected progression-free survival (PFS) as the prognostic end point. The gene expression values were grouped according to the best cut-off values in Kaplan–Meier analysis with R package “survival.” Cox regression was used to analyze the association between PFS and clinicopathologic characteristics in TCGA and the FUSCC cohort. Risk stratification of thyroid cancer recurrence was classified into low, moderate, and high grades according to the American Thyroid Association Guidelines²⁵ and used as a prognostic indicator of FUSCC cohort. Receiver operating characteristic (ROC) curve was used to analyze the ability of THBS1 to predict high recurrence risk.

Quantitative Real-Time PCR (qPCR) and Immunohistochemistry

qPCR was performed on the 53 PTC tissues in the FUSCC cohort, and the $2^{-\Delta\Delta\text{CT}}$ method was used to determine the

relative expression of *THBS1*. For immunohistochemistry (IHC), paraffin sections were prepared from frozen tissue. The Thrombospondin-1 antibody (A6.1, catalogue: NB100-2059, 1:100 dilution) was purchased from Novus Biologicals (Bio-Techne China Co., China). Specimens were scored according to the intensity of staining and the number of positive cells in 5 high magnification views selected at random, and an immunohistochemical score was calculated for each specimen by adding the scores. See Supplemental Appendix 1 for detailed experimental procedures.

Gene Set Enrichment Analysis (GSEA)

Differential gene screening was performed according to *THBS1* expression level using R package “DESeq2” ($|\log_2(\text{FC})| > 1$, $P_{\text{adjust}} < .05$). Gene Ontology (GO) and Kyoto Encyclopedia of Genes and Genomes (KEGG) pathway analyses were performed for differentially expressed genes, and GSEA was performed using the R package “clusterProfile.” Significance was defined as a false discovery rate (FDR) < 0.25 and $P_{\text{adjust}} < .05$.

Establishment of the T-I index

The immune-related gene lists were obtained from ImmPort, and after intersection with former identified *THBS1*-related differentially expressed genes, *THBS1*-immune-related genes were obtained.

Weighted gene co-expression network analysis (WGCNA) was used to identify hub genes with the R package “WGCNA.”²⁶ First, RNA seq data of 503 TCGA tumor samples were used to calculate the Pearson correlation coefficient between 2 genes, and the similarity matrix was constructed. Next, the similarity matrix was transformed into an adjacency matrix with a network type of signed and a soft threshold of $\beta = 3$. The adjacency matrix was converted into a topological overlap matrix to reduce noise and false correlation, and the new distance matrix was obtained. After building the dynamic pruning tree to identify the modules, and setting the module membership (MM) cut-off criteria as $|\text{MM}| > 0.8$,²⁷ hub genes were obtained.²⁷ Genes significantly affecting PFS were identified by Kaplan–Meier analysis and multivariate Cox regression analysis along with *THBS1*. The T-I index score of each sample was calculated by multiplying the expression values of genes and adding the scores together. The coefficient of each gene was determined by its weight in the Cox model. Chord diagram was used to show the relationship between *THBS1* and other genes in T-I index by R package “Circhize.”

Value of T-I index in Prognosis and Immunotherapy Benefit Prediction

The prognosis of different T-I subgroups was evaluated by a nomogram and Kaplan–Meier curves in TCGA cohorts. To validate the independent prognostic value of T-I index, univariate

and multivariate Cox regression analyses were performed. The Tumor Immune Dysfunction and Exclusion (TIDE) score of each sample in TCGA cohort was calculated online (<http://tide.dfci.harvard.edu/>) to predict the likelihood that patients will benefit from immune checkpoint inhibitors (ICI) therapy.^{28,29} ROC curve was used to compare T-I index and single *THBS1* expression level to predict the ability of ICI therapy responder.

Molecular and Immune Characteristics Analysis in Different *THBS1* Expression and T-I Subgroups

To get a more complete insight of the index, we investigated the genetic mutations and immune landscape associated with the index. To analyze the genes mutated in different T-I index subgroups, information on genetic alterations was obtained from the cBioPortal database (<http://www.cbioportal.org/>). The R package “estimate” was used to calculate the Estimation of STromal and Immune cells in MAlignant Tumours using Expression data (ESTIMATE) score of each sample. Single sample GSEA (ssGSEA) was used to analyze the relationship between *THBS1* and 24 classic tumor immune cell subtypes (R package “GSVA”). In addition, the CIBERSORTX (<https://cibersortx.stanford.edu/>) website and the LM22 signature were used to calculate the tumor immune cell infiltration score of each case from TCGA cohort. We then used TIMER (Tumor Immune Estimation Resource) website (<http://timer.cistrome.org/>)^{30–32} and the clinical data from TCGA cohort to screen immune cell subtypes that have a significant impact on the prognosis of thyroid cancer. Spearman was used to analyze the correlation between *THBS1* expression and these immune cells.

Immunofluorescence (IF) staining was performed to determine the infiltration of immune cells in the PTC microenvironment. The CD4 (catalogue: GB13064-1, 1:100 dilution) and FoxP3 (catalogue: GB11093, 1:100 dilution) antibodies were purchased from Servicebio (Servicebio Co., China).

Statistical Analysis

Statistical data acquired from TCGA were merged and converted by R-3.6.3. A P value $< .05$ was set as the cut-off criterion. The R package “pheatmap” was used to draw a tumor-infiltrating immune cell heatmap. The R package “ggplot2” was used for data visualization and image rendering. The Mann–Whitney U -test, Kruskal–Wallis H -test, and Dunn’s test were used for nonparametric tests of independent samples. Wilcoxon signed rank test was used for nonparametric test of paired samples.

Results

THBS1 Expression Level is Correlated with Invasion, Metastasis, and Poor Prognosis of Thyroid Cancer

We obtained clinical and gene expression data of 503 thyroid carcinoma cases, including 503 tumor samples and 58 paired

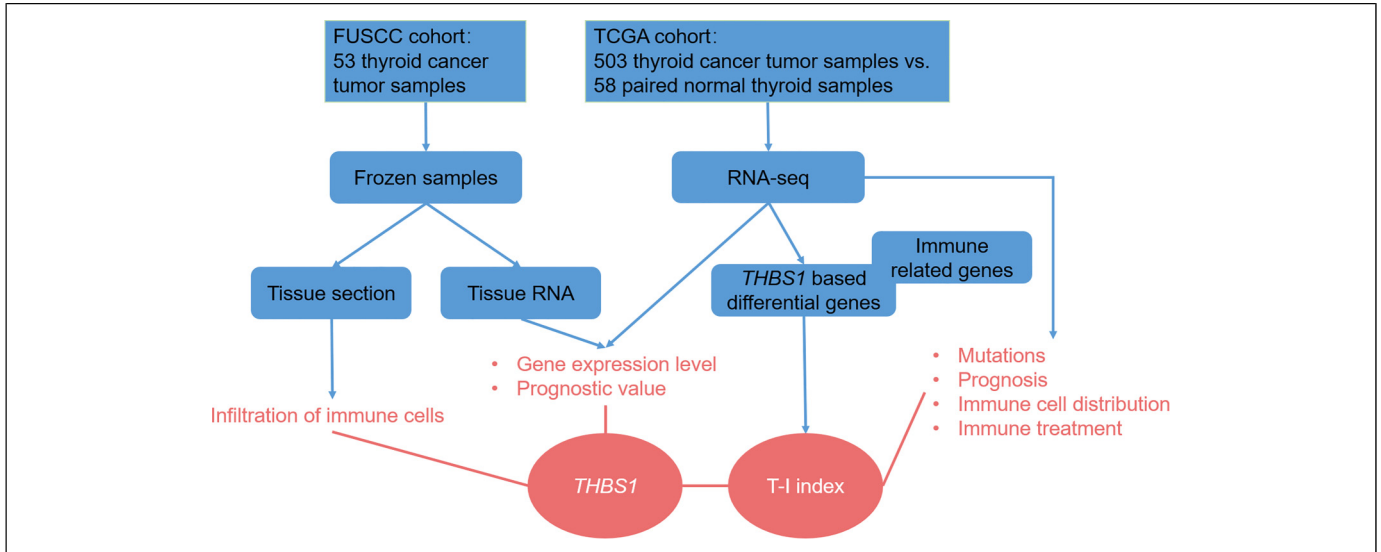


Figure 1. Graphic abstract of this study. *Abbreviations:* TCGA, The Cancer Genome Atlas; FUSCC, Fudan University Shanghai Cancer Center; T-I index, *THBS1*-immune-related gene prognostic index.

normal samples, from TCGA-THCA project. Figure 1 shows a summary of the overall analysis performed in this research. The baseline data of all cases are listed in Supplemental Appendix 2. The *THBS1* expression level in the tumor group was significantly higher than that in the normal group in unpaired samples ($U=0.631$, $P=.005$, Figure 2A and B). However, no significant difference in *THBS1* expression level was detected in the 58 paired samples (Supplemental Appendix 3). There were 357 classical PTC (C-PTC), 101 follicular variant PTC (FV-PTC), 36 tall cell variant PTC (TCV-PTC), and 9 other histological type cases. *THBS1* expression in FV-PTC was lowest, and its expression in TCV-PTC was highest ($P<.001$, Figure 2C). *THBS1* expression in the T3&T4 group was significantly higher than that in the T1&T2 group ($U=0.524$, $P<.001$, Figure 2D). In addition, *THBS1* expression was higher in patients with lymph node metastasis than in patients without lymph node metastasis ($U=0.669$, $P<.001$, Figure 2E). The expression of *THBS1* in the pathological stage III&IV group was significantly higher than that in the stage I&II group ($U=0.45$, $P=.001$, Figure 2F). Furthermore, *THBS1* expression was significantly higher in patients with ETE than in those patients without ETE ($U=0.727$, $P<.001$, Figure 2G).

The cut-off value of *THBS1* expression with the smallest P value was selected and patients were categorized into high and low expression groups using this value. Kaplan–Meier curve analysis revealed that the prognosis of the high *THBS1* expression group ($n=323$) was significantly worse than that of the low *THBS1* expression group ($P=.046$, Figure 2H). However, multivariate Cox regression analysis showed that *THBS1* expression level was not an independent risk factor for the prognosis of thyroid cancer ($P=0.125$, Table 1).

We next examined the expression of *THBS1* in the 53 PTC tissue samples in the validation cohort from FUSCC

(Supplemental Appendix 4). Tumors with high *THBS1* expression showed a larger tumor size ($U=7$, $P=.011$, Figure 2I) and more numbers of lymph node metastases than the low *THBS1* expression group ($U=4$, $P=.002$, Figure 2J). We also observed that with the increase of TNM grade, *THBS1* expression level also increased ($U=3.928$, $P<.001$, Figure 2K). In addition, *THBS1* expression in the samples with ETE was higher than that in the other group ($U=2.285$, $P=.004$, Figure 2L). There were 32 patients at low or moderate recurrence risk, while 21 patients at high recurrence risk. The sensitivity of *THBS1* expression to predict high recurrence risk was 1, and the specificity was 0.719 (area under ROC curve=0.821, Figure 2M). Immunohistochemical staining also showed that *THBS1* protein expression was higher in tumor tissue with a large number of lymph node metastases and ETE (Figure 2N to O). The IHC score of tumor samples was higher than paired normal samples (Figure 2P, $Z=1$, $P=.007$).

MAPK, Tumor Adhesion, and Immune-Related Pathways Enriched in the THBS1 High Expression Phenotype

There were 1826 genes that were differentially expressed according to *THBS1* expression level, including 1320 genes highly expressed in high *THBS1*-expression group and 506 genes expressed at low levels in the low *THBS1*-expression group (Figure 3A). GSEA of data from thyroid cancers with low *THBS1* and high *THBS1* expression was used to identify *THBS1*-related signaling pathways. There were 432 datasets with an FDR (q value) <0.25 and $P_{adj} <.05$. Because of space limitations, we selected several pathways associated with high and low expression to display in Figure 3B. In addition to the classical thyroid cancer-related MAPK, NF- κ B pathway and various tumor-related pathways, *THBS1* expression levels were also associated with many immune-related

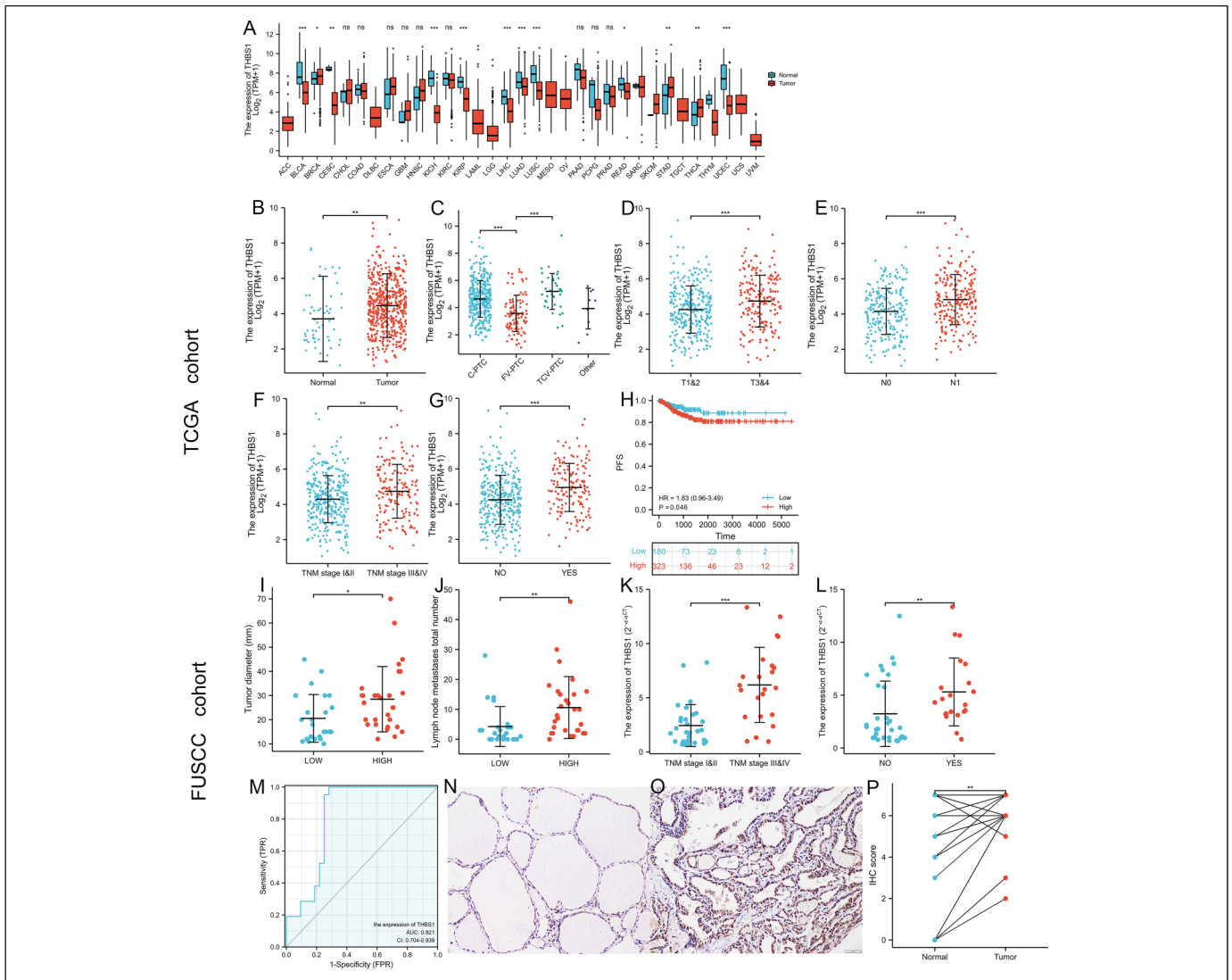


Figure 2. *THBS1* was highly expressed in advanced thyroid cancer. Data in Figure (A) to (H) were from TCGA cohort. (A) Expression of *THBS1* in normal and tumor tissues in different cancer types. (B) The expression level of *THBS1* in the tumor group was higher than that in the normal group. (C) The expression on *THBS1* in FV-PTC was lowest, and it in TCV-PTC was highest. (D) The expression level of *THBS1* in the T1&T2 group was lower than that in the T3&T4 group. (E) *THBS1* expression was higher in patients with lymph node metastasis than in patients without lymph node metastasis. (F) The expression level of *THBS1* in the TNM stage I&II group was lower than that in the stage III&IV group. (G) *THBS1* expression was higher in patients with extrathyroidal extension* than in those who without. (H) Kaplan–Meier survival analysis of *THBS1* expression groups. Data in Figure (I) to (P) were from FUSCC cohort. (I) Tumors with high *THBS1* expression were larger than with low *THBS1* expression. (J) Patients with high *THBS1* expression got more metastatic lymph nodes in the neck. (K) The expression level of *THBS1* in the TNM stage I&II group was lower than that in the III&IV group. (L) *THBS1* expression was higher in patients with extrathyroidal extension* than in those who without. (M) ROC curve for *THBS1* expression level to predict high risk of recurrence. (N to O) Representative images of immunohistochemical staining of *THBS1* protein in normal thyroid and papillary thyroid carcinoma tissue, scale bar: 100 μ m. (P) Comparison of immunohistochemical scores of normal-tumor paired samples. *Abbreviations:* TCGA, The Cancer Genome Atlas; FUSCC, Fudan University Shanghai Cancer Center; ACC, adrenocortical carcinoma; BLCA, bladder urothelial carcinoma; BRCA, breast invasive carcinoma; CESC, cervical squamous cell carcinoma and endocervical adenocarcinoma; CHOL, cholangiocarcinoma; COAD, colon adenocarcinoma; DLBC, lymphoid neoplasm diffuse large B-cell lymphoma; ESCA, esophageal carcinoma; GBM, glioblastoma multiforme; HNSC, head and neck squamous cell carcinoma; KICH, kidney chromophobe; KIRC, kidney renal clear cell carcinoma; KIRP, kidney renal papillary cell carcinoma; LAML, acute myeloid leukemia; LGG, brain lower grade glioma; LIHC, liver hepatocellular carcinoma; LUAD, lung adenocarcinoma; LUSC, lung squamous cell carcinoma; MESO, mesothelioma; OV, ovarian serous cystadenocarcinoma; PAAD, pancreatic adenocarcinoma; PCPG, pheochromocytoma and paraganglioma; PRAD, prostate adenocarcinoma; READ, rectum adenocarcinoma; SARC, sarcoma; SKCM, skin cutaneous melanoma; STAD, stomach adenocarcinoma; TGCT, testicular germ cell tumors; THCA, thyroid carcinoma; THYM, thymoma; UCEC, uterine corpus endometrial carcinoma; UCS, uterine carcinosarcoma; UVM, uveal melanoma; C-PTC, classical papillary thyroid carcinoma; FV-PTC, follicular variant papillary thyroid carcinoma; TCV-PTC, tall cell variant papillary thyroid carcinoma. *, extrathyroidal extension was defined according to 7th American Joint Committee on Cancer guidelines. *, $P < .05$; **, $P < .01$; ***, $P < .001$; ns: not significant.

Table 1. Univariate and Multivariate Cox Regression Analysis of *THBS1* Expression and Thyroid Papillary Cancer Progression-free Survival.

Characteristics	Total (N)	Univariate analysis		Multivariate analysis	
		Hazard ratio (95% CI)	P value	Hazard ratio (95% CI)	P value
Age at initial pathologic diagnosis	503	1.019 (1.003-1.037)	.023	1.018 (1.000-1.037)	.055
Gender	503				
Female	368	Reference			
Male	135	1.535 (0.866-2.719)	.142		
Tumor volume (mm ³)	403	1.011 (1.001-1.022)	.039	1.005 (0.991-1.019)	.476
Primary neoplasm focus type	493				
Unifocal	266	Reference			
Multifocal	227	1.028 (0.591-1.788)	.923		
Primary thyroid gland neoplasm location	497				
Right lobe	213	Reference			
Left lobe	176	1.057 (0.573-1.951)	.859		
Bilateral	86	1.145 (0.523-2.505)	.735		
Isthmus	22	0.409 (0.055-3.044)	.383		
Histological type	503				
C-PTC	357	Reference			
FV-PTC	101	0.601 (0.254-1.422)	.246		
TCV-PTC	36	2.114 (0.942-4.741)	.069		
Other	9	1.060 (0.145-7.727)	.954		
Pathologic stage (T stage)	503				
T1&2	308	Reference			
T3&4	193	2.520 (1.441-4.407)	.001	1.528 (0.585-3.992)	.387
Tx	2	0.000 (0.000-Inf)	.996	0.000 (0.000-Inf)	.998
Pathologic stage (N stage)	503				
N1	224	Reference			
N0	229	0.637 (0.357-1.137)	.127		
Nx	50	0.585 (0.206-1.665)	.315		
Pathologic stage (M stage)	502				
M0	282	Reference			
M1	9	7.767 (2.956-20.412)	<.001	3.731 (1.010-13.790)	.048
Mx	211	1.300 (0.734-2.305)	.368	1.587 (0.847-2.974)	.149
With ETE	485				
No	332	Reference			
Yes	153	2.004 (1.157-3.473)	.013	0.964 (0.385-2.416)	.938
<i>THBS1</i> expression group	503				
Low	180	Reference			
High	323	1.833 (1.06-3.494)	.046	1.735 (0.859-3.506)	.125

C-PTC, classical thyroid papillary cancer; FV-PTC, follicular variant thyroid papillary cancer; TCV-PTC, tall cell variant thyroid papillary cancer; ETE, extrathyroidal extension ETE. Variables with *P* values less than 0.1 in the univariate regression analysis were included in the multivariate regression equation. *P* values less than .05 are indicated in bold.

pathways, such as REACTOME_IMMUNOREGULATORY_INTERACTIONS_BETWEEN_A_LYMPHOID_AND_A_NON_LYMPHOID_CELL and REACTOME_PD_1_SIGNALING pathway. KEGG and GO enrichment analyses were also performed, and several pathways are shown in Figure 3C (the complete GO results are listed in Supplemental Appendix 5). Based on the conditions of *P*.*adj* <.05 and *q* value <0.2, there were 14 pathways in KEGG, 179 pathways in biological process (BP), 14 pathways in cellular component (CC), and 38 pathways in molecular function (MF) subgroups. Similar to the results of GSEA, KEGG and GO analyses also revealed a close relationship between high *THBS1* expression and tumor immunity. The Wnt signaling pathway was found in the enrichment analysis of KEGG, GO and MF. Furthermore,

cell adhesion, integrin binding, and other pathways were related to high *THBS1* expression.

High Expression of *THBS1* Suppresses the Anti-Tumor Immune Microenvironment

The enrichment analysis results suggested that *THBS1* expression level may be related to immune molecules and immune pathways. Therefore, we examined whether *THBS1* expression was associated with immune infiltration in thyroid cancer. We first calculated the ESTIMATE score of each sample to reflect the tumor immunity score and tumor purity. As shown in Figure 4A, *THBS1* expression was positively correlated with both stromal score and immune score, indicating that patients

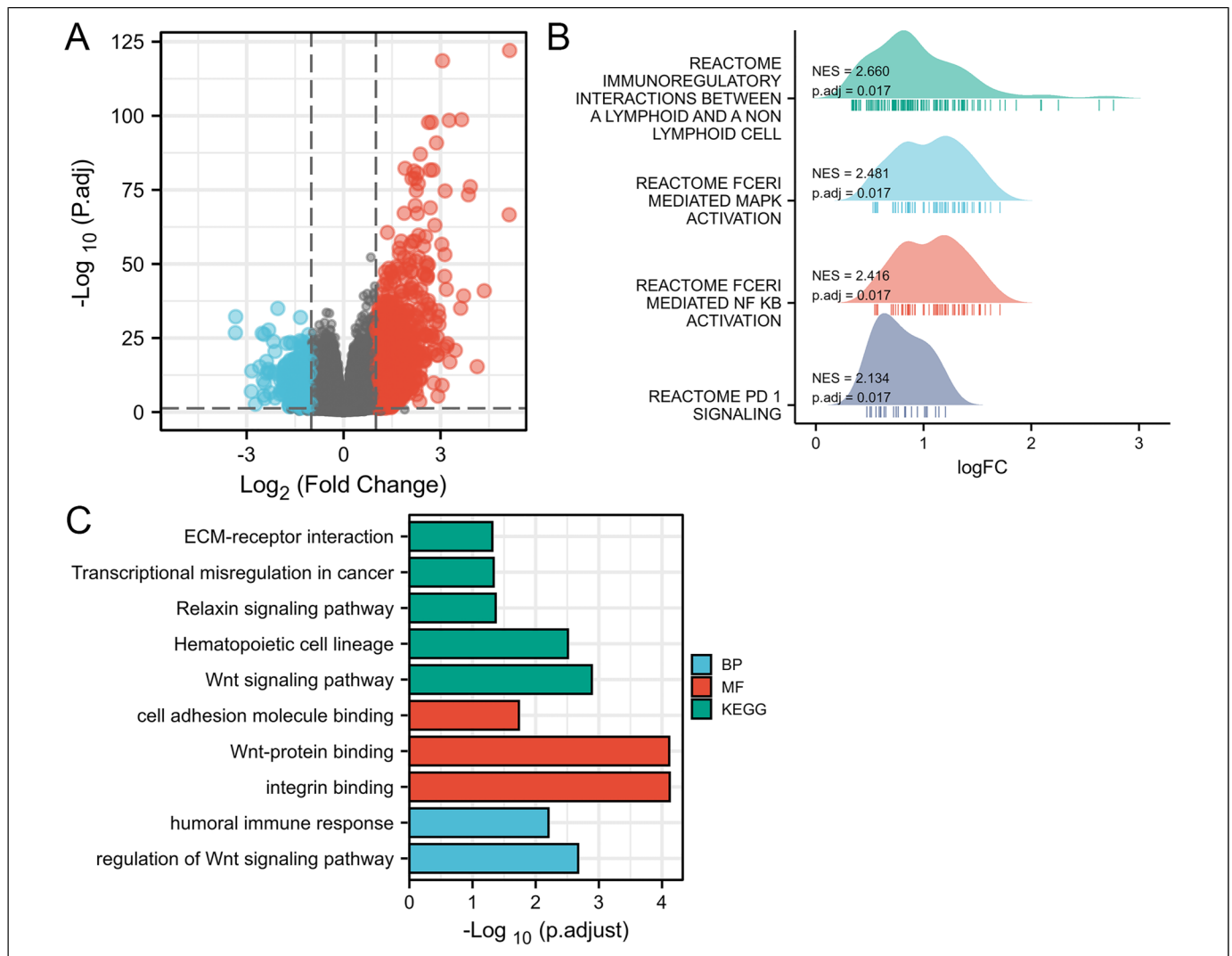


Figure 3. THBS1-related signaling pathways based on GSEA and GO enrichment analysis. (A) Differentially expressed genes associated with THBS1 expression. 1826 genes met $|\log_2(\text{FC})| > 1$ and $P_{\text{adj}} < .05$ threshold value including 1320 high expression genes (log FC positive, red points) and 506 low expression genes (log FC negative, blue points). (B) Four noteworthy signaling pathways THBS1-related signaling pathways based on GSEA. (C) 10 noteworthy signaling pathways THBS1-related signaling pathways based on KEGG, MF, and BP.

Abbreviations: FC, fold change; GSEA, gene set enrichment analysis; KEGG, Kyoto Encyclopedia of Genes and Genomes; MF, molecular function; BP, biological process.

with higher *THBS1* expression level had more stromal cells and immune cells infiltrated in TME ($P < .001$). We then used ssGSEA to analyze the relationship between *THBS1* expression and 24 classic tumor immune cell subtypes (Figure 4B). We found that *THBS1* expression was positively correlated with the level of infiltration of most of the immune cells. We also used CIBERSORTx to analyze the level of immune cell infiltration of each sample in TCGA cohort with the LM22 signature for classification. The proportions of 22 types of immune cells in different *THBS1* expression groups are shown in Figure 4C. Based on the results of these 2 analyses, we concluded that *THBS1* expression level was correlated with T cell infiltration level of different subtypes. Therefore, we used TIMER website and clinical data from TCGA cohort to screen immune cells that could affect the prognosis of

thyroid cancer. We found that high fractions of follicular helper T cells (TFH) and regulatory T cells (Tregs) were significantly associated with shorter progression-free interval (PFI) in thyroid cancer (TFH: HR = 3.02, $P = 0.011$, Tregs: HR = 2.88, $P = .009$, Figures 4D and E). Furthermore, Figures 4F and G show the positive relationship between *THBS1* expression level and TFH and Tregs infiltration, indicating that high expression of *THBS1* might lead to a poorer outcome in thyroid cancer via suppressing the anti-tumor immune microenvironment.

We performed IF staining of tissue sections from patients in the FUCSS cohort to show Tregs infiltration in papillary thyroid carcinoma. As shown in Figure 5, in samples with high *THBS1* expression, there was a high infiltration of CD4-positive/FoxP3-positive Tregs in the tumor tissue.

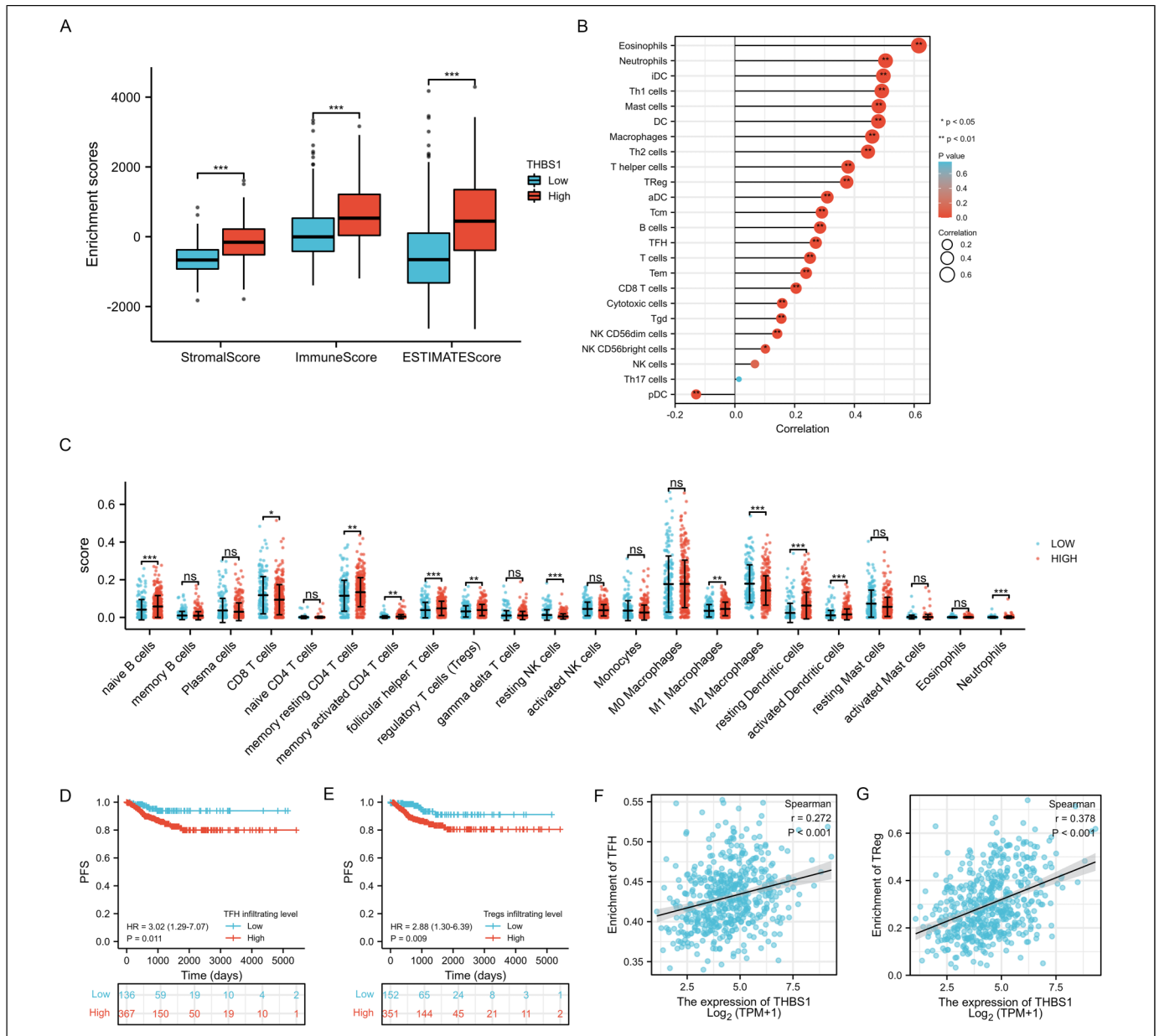


Figure 4. Relationship between *THBS1* expression and tumor-infiltrating immune cells. (A) Tumor immunity score according to *THBS1* expression group using ESTIMATE algorithm. Correlation analysis between *THBS1* expression and ESTIMATE score. Tumors with high *THBS1* expression got higher stromal, immune, and ESTIMATE score ($P < .001$). (B) Relationship between *THBS1* expression and 24 subtypes of tumor-infiltrating immune cells according to ssGSEA method. (C) The infiltrating level of immune cells in different *THBS1* expression groups according to CIBERSORTx and LM22 signature. (D to E). Kaplan–Meier survival analysis of TFH and Tregs infiltrating level groups (HR = 3.02, $P = 0.011$, HR = 2.88, $P = .009$). (F to G). Correlation analysis results between *THBS1* expression and immune cell infiltration fraction according to ssGSEA: TFH ($r = 0.27$, $P < .001$); Tregs ($r = 0.380$, $P < .001$). ssGSEA, single sample gene set enrichment analysis; ESTIMATE, estimation of stromal and immune cells in malignant tumors using expression data; TFH, follicular helper T cells, Tregs, regulatory T cells. ns, not significant. *, $P < .05$; **, $P < .01$; ***, $P < .001$.

THBS1-Immune-Related Hub Genes and a Prognostic index

Since high *THBS1* expression level is not an independent risk factor for PFS in thyroid cancer, we then designed a *THBS1*-immune-related gene prognostic index. We examined differentially expressed genes between 323 high *THBS1* expression

cases and 180 low *THBS1* expression cases, and a total of 1826 differentially expressed genes were obtained. After intersecting these genes with the list of immune-related genes acquired from ImmPort, a total of 292 *THBS1*-immune-related genes were selected for WGCNA (Figure 6A). The optimal soft-thresholding power was 3 based on the scale-free network (Supplemental Appendix 6A-B). A total of 75 hub genes and 3 modules were

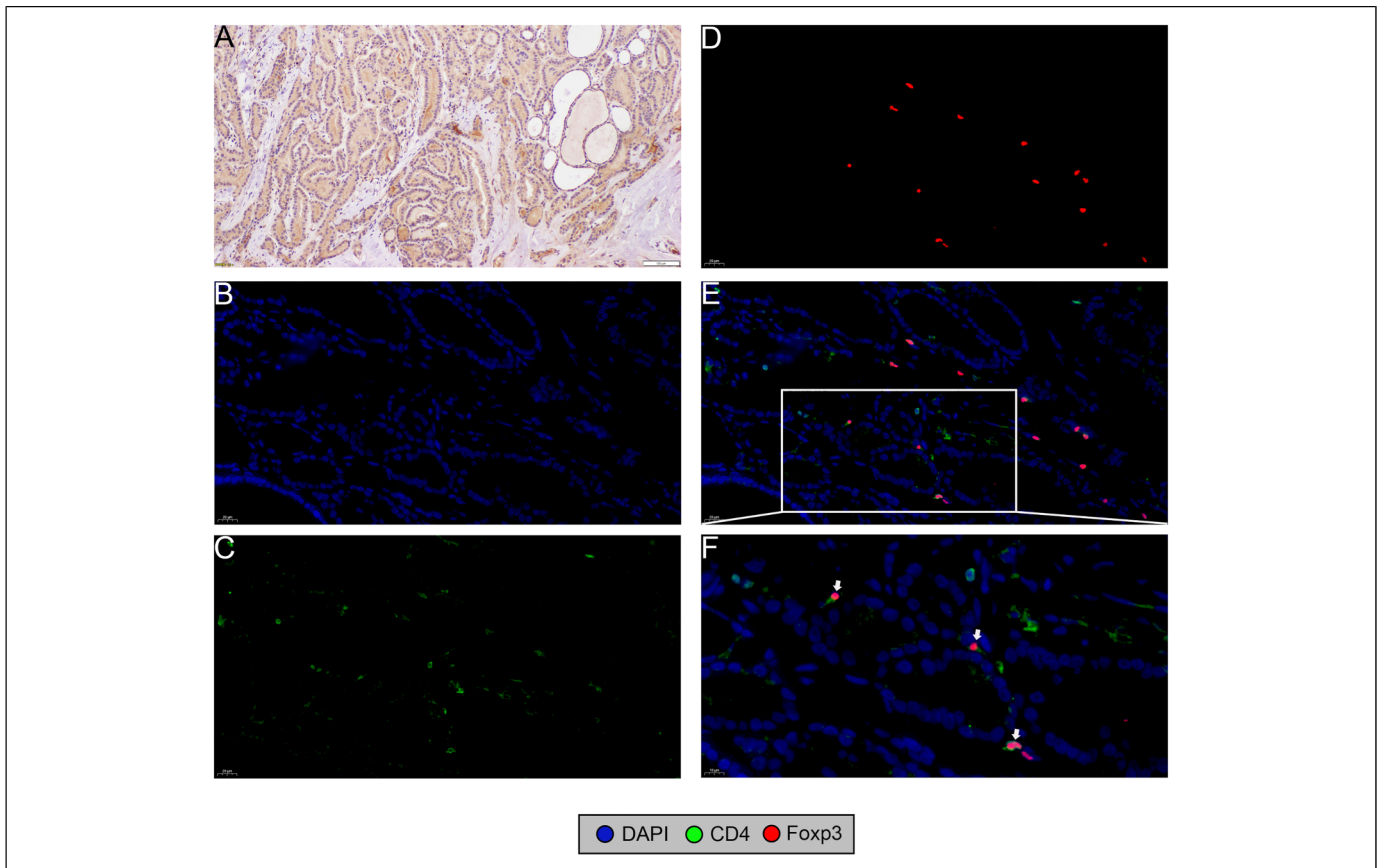


Figure 5. Immunofluorescence staining for Tregs infiltration in high *THBS1*-expressing samples. (A) Representative image of immunohistochemical staining of *THBS1* protein in a high *THBS1*-expression papillary thyroid carcinoma tissue, scale bar: 100 μ m. (B to F) Immunofluorescence staining of Tregs from the same sample (scale bar in B to E: 20 μ m, scale bar in F: 10 μ m). Arrows point to CD4-positive/FoxP3-positive co-localized Tregs.

allocated (30 genes in module blue, 5 genes in module brown, 40 genes in module turquoise, 1 gene in module grey, Supplemental Appendix 6C-D). Because of the small number of hub genes screened, we did not conduct phenotypic correlation analysis on these 3 modules. However, we did perform Kaplan–Meier analysis to identify the genes that correlated with the PFS of thyroid cancer. Twelve genes were significantly associated with PFS, and their expression levels were grouped according to the optimal cut-off value. Multivariate Cox regression analysis was performed, and 4 genes along with *THBS1* were identified for index construction with their coefficient in the Cox model. The *THBS1*-immune-related gene prognostic index was calculated by the formula = expression level of *IGHV3-49* *0.18 + expression of *CXCL13* *0.006 + *TRAV8-3* *0.3 + expression of *TRBV30* *0.22 + expression of *THBS1* *0.45. Figure 6B shows the co-expression heatmap of *THBS1* and these 4 genes, and Figure 6C shows the relationship between them. A flow chart showing the establishment of the *THBS1*-immune-related gene prognostic index is depicted in Supplemental Appendix 6E, and Kaplan–Meier curves of 4 selected genes are shown in Figure 6D-G.

Univariate and multivariate Cox analyses indicated that high T-I index score was an independent risk factor for shorter PFI in thyroid cancer (hazard ratio = 2.738, $P = .025$, Table 2). A nomogram of clinical characteristics and T-I index group is shown Figure 7A. Patients in the high T-I subgroup had a significantly shorter PFI than those in the low T-I subgroup ($P = .035$, Figure 7B). TIDE website provides an online ICI therapy benefit prediction algorithm including dysfunction and exclusion score to reflect the dysfunction and exclusion of T cells. Higher TIDE score represented a higher potential for immune evasion, which suggested that the patients were less likely to benefit from ICI therapy. According to the Wilcoxon test, both dysfunction and exclusion scores in the high T-I index subgroup were higher than those in the low subgroup (Figure 7C), indicating that patients with a higher T-I index score may be more likely to benefit from ICI therapy. According to TIDE results, there were 426 potential responders to ICI therapy (Supplemental Appendix 7). The distribution of different histological subtypes of PTC in T-I index groups and TIDE responder groups is shown in the Appendix. Compared with *THBS1* expression alone, the T-I

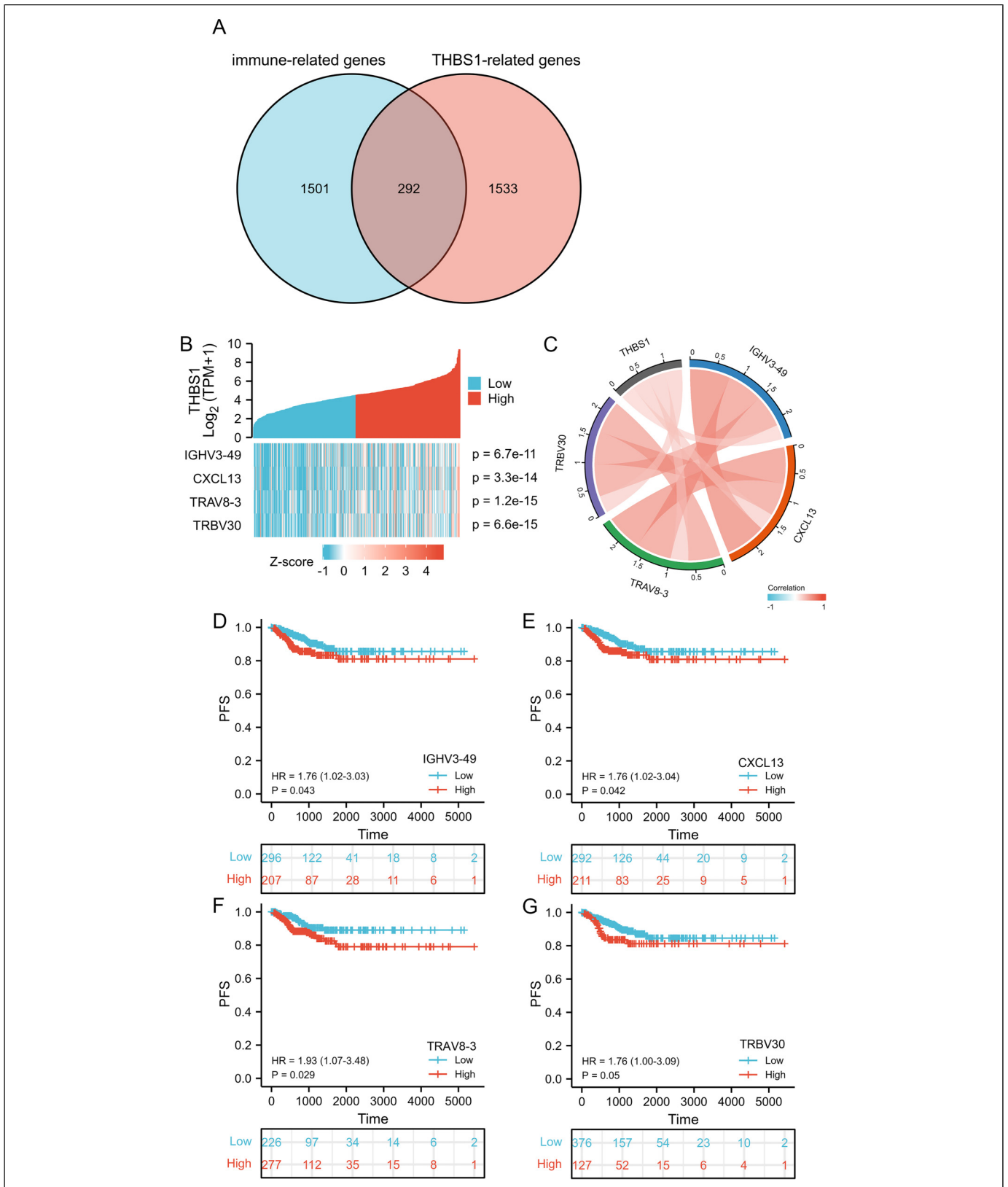


Figure 6. Design of *THBS1*-immune-related gene prognostic index and K-M plots of 4 selected genes. (A) Venn diagram of 1826 *THBS1*-related genes and 1793 immune-related genes with 292 genes in intersection region. (B) Co-expression heatmap of *THBS1* and other 4 T-I index genes obtained from WGCNA (Spearman analysis, $P < .001$). (C) Chord diagram of *THBS1* and other 4 T-I index genes. The red circle arc represented 2 genes were positively correlated. (D to G) Kaplan–Meier survival analysis of 4 selected genes significant in the univariate Cox analysis ($P \leq .05$). T-I index, *THBS1*-immune-related gene prognostic index; WGCNA, weighted gene co-expression network analysis.

Table 2. Univariate and Multivariate Cox Regression Analysis of T-I Index and Thyroid Papillary Cancer Progression-free Survival.

Characteristics	Total(N)	Univariate analysis		Multivariate analysis	
		Hazard ratio (95% CI)	<i>P</i> value	Hazard ratio (95% CI)	<i>P</i> value
Age at initial pathologic diagnosis	503	1.019 (1.003-1.037)	.023	1.019 (1.001-1.038)	.043
Gender	503				
Male	135	Reference			
Female	368	0.651 (0.368-1.154)	.142		
Tumor volume (mm ³)	403	1.011 (1.001-1.022)	.039	1.006 (0.992-1.019)	.410
Primary neoplasm focus type	493				
Unifocal	266	Reference			
Multifocal	227	1.028 (0.591-1.788)	.923		
Primary thyroid gland neoplasm location	497				
Right lobe	213	Reference			
Left lobe	176	1.057 (0.573-1.951)	.859		
Bilateral	86	1.145 (0.523-2.505)	.735		
Isthmus	22	0.409 (0.055-3.044)	.383		
Histological type	503				
C-PTC	357	Reference			
FV-PTC	101	0.601 (0.254-1.422)	.246		
TCV-PTC	36	2.114 (0.942-4.741)	.069		
Other	9	1.060 (0.145-7.727)	.954		
Pathologic stage (t stage)	503				
T1&2	308	Reference			
T3&4	193	2.520 (1.441-4.407)	.001	1.550 (0.590-4.074)	.374
Tx	2	0.000 (0.000-Inf)	.996	0.000 (0.000-Inf)	.998
Pathologic stage (n stage)	503				
N0	229	Reference			
N1	224	1.569 (0.880-2.798)	.127		
Nx	50	0.918 (0.312-2.700)	.877		
Pathologic stage (m stage)	502				
M0	282	Reference			
M1	9	7.767 (2.956-20.412)	<.001	4.264 (1.162-15.652)	.029
Mx	211	1.300 (0.734-2.305)	.368	1.648 (0.882-3.082)	.118
With ETE	486				
No	332	Reference			
Yes	153	2.004 (1.157-3.473)	.013	0.946 (0.377-2.372)	.905
T-I index	503				
Low	134	Reference			
High	369	2.353 (1.061-5.217)	.035	2.738 (1.133-6.616)	.025

C-PTC, classical thyroid papillary cancer; FV-PTC, follicular variant thyroid papillary cancer; TCV-PTC, tall cell variant thyroid papillary cancer; ETE, extrathyroidal extension ETE. Variables with *P* values less than .1 in the univariate regression analysis were included in the multivariate regression equation. *P* values less than .05 are indicated in bold.

index exhibited a better ability to screen these responders (Figure 7D).

Molecular and Immune Characteristics of Different T-I Subgroups

To gain a complete insight into T-I index, we first analyzed gene mutations in different T-I subgroups using data from cBioPortal database. Missense mutation was the most common mutation type in both high and low T-I subgroups. The 15 genes with the highest mutation rates in all cases are listed in Figure 8A. *BRAF* was the most common mutated gene and showed the biggest difference in expression between high and low T-I subgroups ($P < .001$). While *NRAS* mutation occurred more in the low T-I group ($P < .001$).

A heatmap of tumor immune cell infiltrating score from 503 thyroid cancer samples in TCGA cohort according to CIBERSORTx is shown in Figure 8B, with *THBS1* expression level and T-I index grouping as patient annotations. Similar to the above results, we found that TFH and Tregs were more abundant in the high T-I subgroup (Figure 8C). Therefore, we speculated that the prognostic value of T-I index might result from both worse immune control and more aggressive cancer growth.

Discussion

THBS1 exhibits various roles in different tumors.¹⁵ Previous studies showed that *THBS1* not only promotes tumor invasion and metastasis in PTC,³³ but also inhibits angiogenesis in early PTC.³⁴ *THBS1* also regulates resistance to anaplastic thyroid

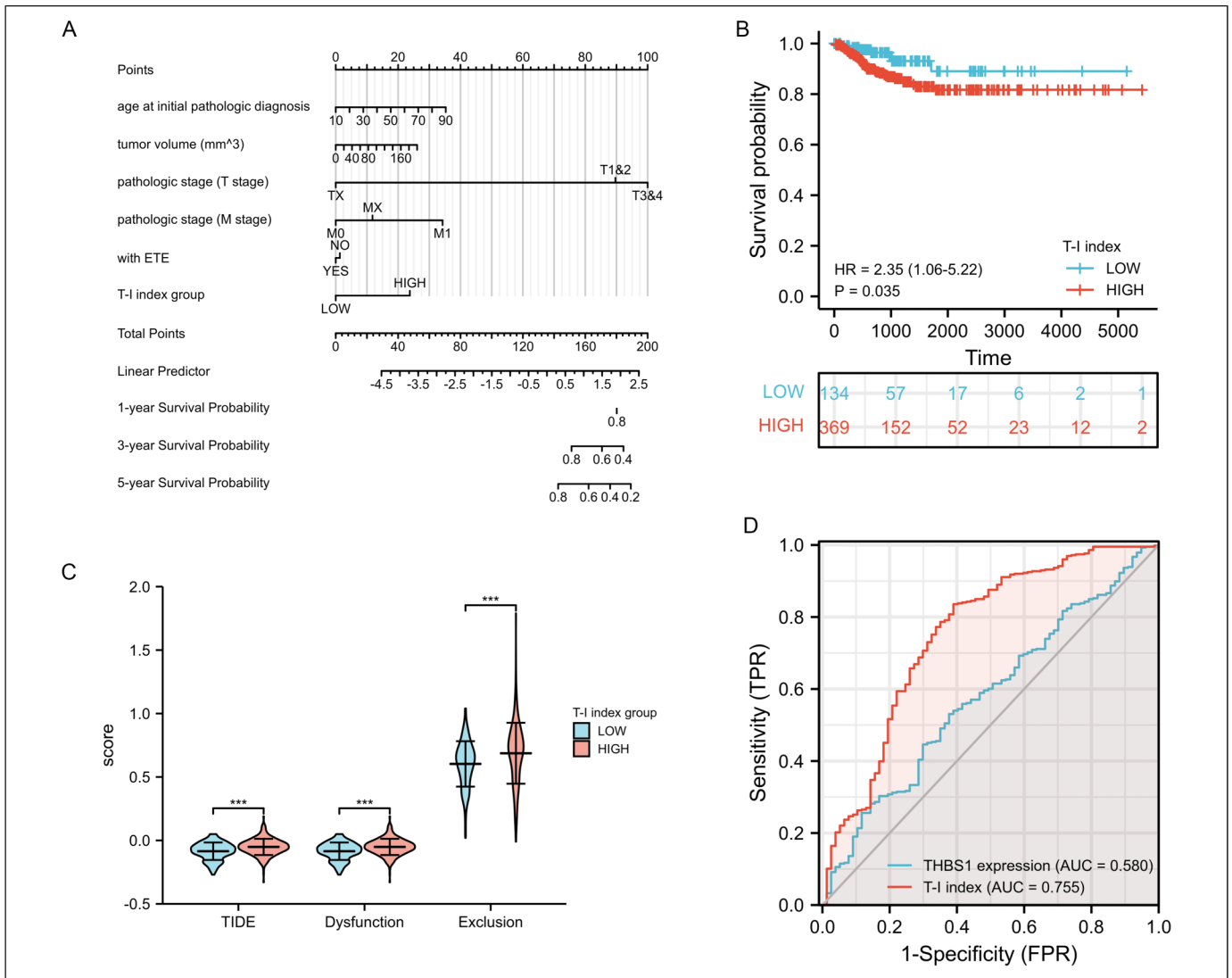


Figure 7. Prognosis analysis of different T-I subgroups and the prognostic value of T-I index in patients with immune therapy. (A) Nomogram of clinical characteristics and T-I index group. (B) Kaplan–Meier survival analysis of T-I index groups. (C) The TIDE, dysfunction and exclusion score in different T-I index groups. (D) ROC curve of T-I index groups and single THBS1 expression groups to predict the responder of immune checkpoint suppression therapy according to the TIDE results. TIDE, the tumor immune dysfunction and exclusion score. ***, $P < .001$.

carcinoma-targeted therapy.³⁵ Therefore, the various roles of THBS1 in thyroid cancer deserve further elucidation.

In our research, analyses of TCGA cases showed that *THBS1* expression level was higher in the thyroid tumor group compared with the normal group. Given the high positive correlation between THBS1 expression level and higher tumor pathological stage, lymph node metastasis, and ETE, we speculate that THBS1 plays an important role in tumor invasion and metastasis in PTCs. For the validation cohort from FUSCC, 53 paired frozen specimens were acquired from the tissue bank department. High *THBS1* expression was positively correlated with a larger tumor size, higher TNM stage, more lymph node metastasis, and ETE. Although patients with higher THBS1 expression level showed a shorter PFI in TCGA cohort, *THBS1* expression was not an independent risk factor in multivariate Cox regression analysis. Because of the short

follow-up time of the FUSCC cohort, we analyzed the ability of *THBS1* expression to predict high cancer recurrence risk. These results indicate that high expression of *THBS1* in advanced thyroid cancer is associated with tumor invasion and metastasis, but its value as an independent prognostic biomarker is limited.

From the gene enrichment results, we identified a correlation between *THBS1* expression and MAPK pathway. The activation of MAPK pathway is closely related to the occurrence and poor outcome of thyroid cancer.³⁶ Previous studies have shown that inhibition of *THBS1* expression can reduce the phosphorylation levels of ERK and MEK, thus inhibiting the invasion and metastasis of PTC.³³ Therefore, we speculated that the high expression of *THBS1* may promote cancer by promoting the activation of MAPK pathway. PD1 is a classic immune checkpoint molecule, and closely related to the role

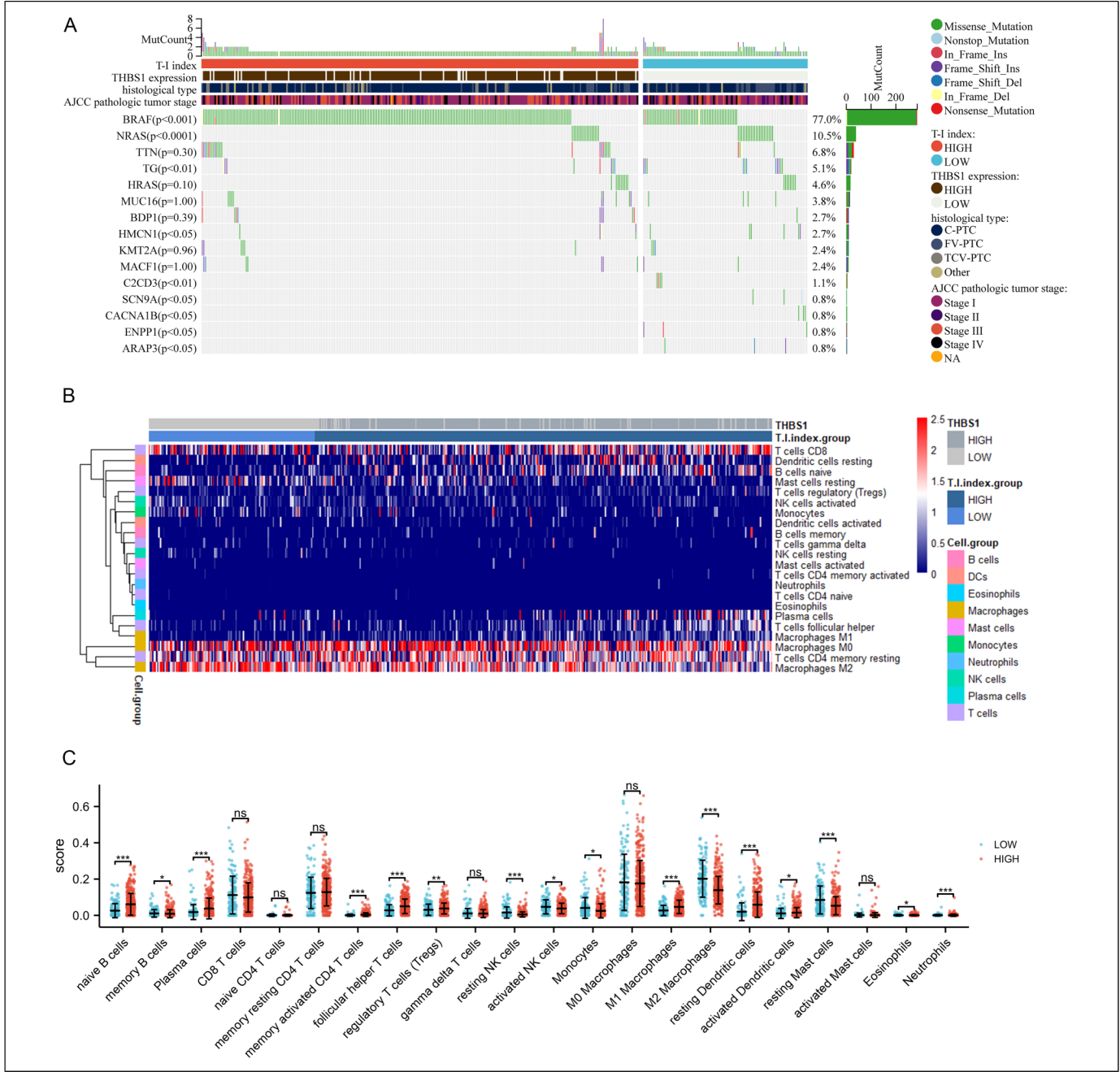


Figure 8. Molecular characteristics and TME landscape in different T-I subgroups. (A) Significantly mutated genes in the mutated TCGA-THCA cohort samples of different T-I subgroups. (B) Heatmap of tumor immune cell infiltrating score from 503 thyroid cancer samples in TCGA. Cases were divided into the HIGH and LOW groups according to the expression level of *THBS1* and T-I index score. Cases are displayed on the X-axis; the Y-axis is clustered according to the immune cell subpopulation and infiltration fraction. (C) The proportions of 22 subpopulations of immune cells in different T-I index subgroups. The scattered dots represent the immune score of the 2 subgroups, and the score between them were compared through the Wilcoxon test. ns, not significant; *, $P < .05$; **, $P < .01$; ***, $P < .001$.

of T cells in tumor immunity. The enrichment of PD1 pathway in the high *THBS1* expression group also suggested that the high expression of *THBS1* may be closely related to tumor immunosuppression. Furthermore, KEGG and GO enrichment analysis results showed that the Wnt signaling pathway was enriched in the *THBS1* high expression group. This signaling pathway is related to ETE, epithelial-mesenchymal

transformation, tumor immunosuppression, and drug resistance in thyroid cancer.³⁷⁻³⁹ In addition, MF enrichment analysis showed that high *THBS1* expression was associated with tumor adhesion, which was consistent with previous findings in breast cancer.¹⁹ We also found that the integrin-binding pathway was enriched in the group with high *THBS1* expression. Therefore, we performed immunohistochemical analysis

of clinical specimens for co-expression of the neovascular marker CD31 and THBS1. However, we did not find clear evidence of THBS1 inhibiting neovascularization in thyroid cancer (data not shown). This result was not in line with findings from a previous study.³⁴

The prognosis of thyroid cancer, especially PTCs, is good and most of them can be cured by surgical resection. However, a few patients with advanced PTCs may be lost to surgery because of reasons such as huge neck masses, and immunotherapy may provide a new treatment option for these patients. Several studies have demonstrated higher levels of immune cell infiltration in PTC than in normal thyroid tissue, suggesting that PTC patients may benefit from immunotherapy.^{40,41} Studies on how key genes in PTCs regulate its immune microenvironment have also been reported in the literature. For example, inhibition of *BRAF* sensitizes thyroid carcinoma to immunotherapy by enhancing MHCII-mediated immune recognition.⁴² In addition, in a trial of pediatric PTCs, investigators found that gene-fusion-driven PTCs were less differentiated and associated with more overrepresentation of mutations in tumor-immune crosstalk pathways.⁴³ Therefore, we suggest that some genes that affect prognosis in PTCs may act simultaneously by regulating the immune microenvironment.⁴⁴ It is essential to analyze such genes or molecular markers in conjunction with their relationship with tumor immunity.

Previous studies have examined the role of THBS1 in tumor immunity,^{23,45} and our latest imaging histology study also found THBS1 is related to the tumor immunity-related pathways. However, the role for THBS1 in tumor immunity in thyroid cancer has not been studied. We first calculated the stromal score and immune score in different *THBS1* expression groups using ESTIMATE. The higher ESTIMATE score in high *THBS1* expression group indicated more immune cells in the TME. We then used ssGSEA and CIBERSORTx to analyze the tumor-infiltrating immune cells related to *THBS1* expression in thyroid cancer. Both ssGSEA and CIBERSORTx results showed that the expression level of *THBS1* was correlated with multiple immune cell subtypes, especially T cells. However, not all types of immune cells played a key role in the prognosis of thyroid cancer. Therefore, we further examined the association of immune cells with PFS using the TIMER website and clinical data from TCGA cohort. We found that TFH and Tregs infiltration were positively correlated with poor outcome in thyroid cancer. Given that high expression of *THBS1* was positively correlated with the infiltration level of TFH and Tregs, we speculate that THBS1 may play a role in tumor immunosuppression via regulating these 2 types of immune cells.

Since the ability of *THBS1* expression alone as a prognostic biomarker was limited, we next constructed a multigene prediction index with *THBS1* and immune-related genes to improve the efficacy of THBS1 in prognosis prediction. After WGCNA, 4 THBS1-immune-related genes that significantly affected prognosis in thyroid cancer were selected to build the T-I index. Patients with a higher T-I index score showed a shorter PFI, and T-I index was proven to be an independent

risk factor in multivariate Cox analysis. Furthermore, patients with a higher T-I index score showed a higher TIDE score including both Dysfunction score and Exclusion score, indicating that they are less likely to be the responder in ICI therapy. Therefore, the T-I index can also be used to predict the possibility of immunotherapy benefit.

The T-I index consists of 5 genes: *IGHV3-49*, *CXCL13*, *TRAV8-3*, *TRBV30*, and *THBS1*. C-X-C motif chemokine ligand 13 (*CXCL13*) is a well-known cancer-related gene. *CXCL13* and its receptor *CXCR5* (C-X-C motif chemokine receptor 5) are highly expressed in various tumors.^{46,47} Overabundance of CD4(+) *CXCR5*(+) follicular helper T cells in thyroid cancer promoted tumor metastasis.⁴⁸ This conclusion is consistent with the results that high *THBS1* expression level positively correlated with TFH infiltration and led to a shorter PFI as described above. *IGHV3-49* (immunoglobulin heavy variable 3-49) is a member of the IGHV family and mainly associated with B cell immunity and chronic lymphocytic leukemia.⁴⁹ *TRAV8-3* and *TRBV30* belong to T cell receptor alpha and beta subgroups and directly affect T cell immunity. In a study of T cell receptors in patients with goiter cancer, the proportion of TRBV in tumor tissue, peripheral blood, and lymphocytes varied, supporting further study of immunity mechanisms against PTC.⁵⁰ In the calculation formula of T-I index, the coefficient of these genes and *THBS1* were positive numbers, indicating a positive correlation between T-I index and these genes. These findings indicate that T-I index is a biomarker associated with tumor promotion and tumor immunity suppression.

To obtain a complete insight of the T-I index, we then analyzed the gene mutation situation in different T-I subgroups with cBioPortal dataset. *BRAF* was the top mutated gene (77% mutation count) and most occurred in the high T-I group ($P < .001$). Notably, *BRAF* is the most common gene mutated in thyroid cancer, especially PTCs, and has been proven to be an important prognostic biomarker.⁵¹ The high *BRAF* mutation rate in the high T-I group may be due to the higher prevalence of C-PTC in this subgroup and be responsible for the poorer prognosis. In contrast, the higher mutation rate of *NRAS* in the low T-I group may have originated from the fact that FV-PTC was mainly concentrated in this group. This subtype is characterized by both papillary and follicular carcinoma molecular landscapes and therefore exhibits more *NRAS* mutations characteristic of follicular carcinoma.⁵² We also used the results of CIBERSORTx to analyze the immune characteristics in different T-I subgroups. Similar to result in the *THBS1* expression level group, there were more TFH and Tregs infiltrations in the high T-I index group. As shown in the heatmap in Figure 6, some cases with low *THBS1* expression were categorized into the high T-I subgroup. This is equivalent to a decrease in “false negative cases.” Thus, the T-I index showed effectiveness at predicting the benefit of immunotherapy.

The main shortcoming of this study is the short follow-up time in the validation cohort. In addition, we did not conduct gene sequencing on the validation cohort, so we could not

obtain the absolute expression value of each gene or verify the infiltration of immune cells. In addition, to maintain consistency in the analysis of clinical information of patients in this study, we used the ETE and TNM grading criteria of the 7th edition of the AJCC guidelines, which is different from how the latest 8th edition of the guidelines grade ETE and tumors, which may lead to insufficient evidence of the correlation between THBS1 and ETE.

Conclusion

THBS1 is highly expressed in thyroid cancer, especially high-grade thyroid cancer. High *THBS1* expression is associated with a shorter PFI and tumor immunosuppression. The T-I index is a valid prognostic biomarker for outcome and immunotherapy benefit in thyroid cancer.

Declaration of Conflicting Interests

The authors declared no potential conflicts of interest with respect to the research, authorship, and/or publication of this article.

Funding

The authors disclosed receipt of the following financial support for the research, authorship, and/or publication of this article: This study received funding from the National Natural Science Foundation of China (No.: 82071945).

Ethical Disclosure

All research protocols were approved by the ethical committee of Fudan University Shanghai Cancer Center (approval 2101-ZZK-41) and all enrolled patients signed informed consent forms.

ORCID iD

Cai Chang  <https://orcid.org/0000-0001-7996-765X>

Supplemental Material

Supplemental material for this article is available online.

References

- Siegel RL, Miller KD, Jemal A. Cancer statistics, 2020. *CA Cancer J Clin*. 2020;70(1):7-30. doi:10.3322/caac.21590
- Shaha AR, Migliacci JC, Nixon IJ, et al. Stage migration with the new American joint committee on cancer (AJCC) staging system (8th edition) for differentiated thyroid cancer. *Surgery*. 2019;165(1):6-11. doi:10.1016/j.surg.2018.04.078
- Roman BR, Morris LG, Davies L. The thyroid cancer epidemic, 2017 perspective. *Curr Opin Endocrinol Diabetes Obes*. 2017;24(5):332-336. doi:10.1097/med.0000000000000359
- Raue F, Frank-Raue K. Thyroid cancer: risk-stratified management and individualized therapy. *Clin Cancer Res: Off J Am Assoc Cancer Res*. 2016;22(20):5012-5021. doi:10.1158/1078-0432.Ccr-16-0484
- Ibrahimovic T, Ghossein R, Shah JP, Ganly I. Poorly differentiated carcinoma of the thyroid gland: current status and future prospects. *Thyroid*. 2019;29(3):311-321. doi:10.1089/thy.2018.0509
- Gonzalez H, Hagerling C, Werb Z. Roles of the immune system in cancer: from tumor initiation to metastatic progression. *Genes Dev*. 2018;32(19-20):1267-1284. doi:10.1101/gad.314617.118
- Yang SR, Tsai MH, Hung CJ, et al. Anaplastic thyroid cancer successfully treated with radiation and immunotherapy: a case report. *AACE Clin Case Rep*. 2021;7(5):299-302. doi:10.1016/j.aace.2021.03.003
- Gunda V, Gigliotti B, Ndishabandi D, et al. Combinations of BRAF inhibitor and anti-PD-1/PD-L1 antibody improve survival and tumour immunity in an immunocompetent model of orthotopic murine anaplastic thyroid cancer. *Br J Cancer*. 2018;119(10):1223-1232. doi:10.1038/s41416-018-0296-2
- Sun J, Shi R, Zhang X, et al. Characterization of immune landscape in papillary thyroid cancer reveals distinct tumor immunogenicity and implications for immunotherapy. *Oncoimmunology*. 2021;10(1):e1964189. doi:10.1080/2162402x.2021.1964189
- Lin P, Guo YN, Shi L, et al. Development of a prognostic index based on an immunogenomic landscape analysis of papillary thyroid cancer. *Aging (Albany NY)*. 2019;11(2):480-500. doi:10.18632/aging.101754
- Wolf FW, Eddy RL, Shows TB, Dixit VM. Structure and chromosomal localization of the human thrombospondin gene. *Genomics*. 1990;6(4):685-691. doi:10.1016/0888-7543(90)90505-o
- Adams JC. Thrombospondin-1. *Int J Biochem Cell Biol*. 1997;29(6):861-865. doi:10.1016/s1357-2725(96)00171-9
- Lawler PR, Lawler J. Molecular basis for the regulation of angiogenesis by thrombospondin-1 and -2. *Cold Spring Harb Perspect Med*. 2012;2(5):a006627. doi:10.1101/cshperspect.a006627
- Maxhimer JB, Soto-Pantoja DR, Ridnour LA, et al. Radioprotection in normal tissue and delayed tumor growth by blockade of CD47 signaling. *Sci Transl Med*. 2009;1(3):3ra7. doi:10.1126/scitranslmed.3000139
- Wang P, Zeng Z, Lin C, et al. Thrombospondin-1 as a potential therapeutic target: multiple roles in cancers. *Curr Pharm Des*. 2020;26(18):2116-2136. doi:10.2174/1381612826666200128091506
- Qian X, Rothman VL, Nicosia RF, Tuszynski GP. Expression of thrombospondin-1 in human pancreatic adenocarcinomas: role in matrix metalloproteinase-9 production. *Pathol Oncol Res*. 2001;7(4):251-259. doi:10.1007/bf03032381
- Albo D, Berger DH, Wang TN, Hu X, Rothman V, Tuszynski GP. Thrombospondin-1 and transforming growth factor-beta 1 promote breast tumor cell invasion through up-regulation of the plasminogen/plasmin system. *Surgery*. 1997;122(2):493-499. doi:10.1016/s0039-6060(97)90043-x. discussion 499-500.
- Albo D, Rothman VL, Roberts DD, Tuszynski GP. Tumour cell thrombospondin-1 regulates tumour cell adhesion and invasion through the urokinase plasminogen activator receptor. *Br J Cancer*. 2000;83(3):298-306. doi:10.1054/bjoc.2000.1268
- Horiguchi H, Yamagata S, Rong Qian Z, Kagawa S, Sakashita N. Thrombospondin-1 is highly expressed in desmoplastic components of invasive ductal carcinoma of the breast and associated with lymph node metastasis. *J Med Invest*. 2013;60(1-2):91-96. doi:10.2152/jmi.60.91

20. Sid B, Langlois B, Sartelet H, Bellon G, Dedieu S, Martiny L. Thrombospondin-1 enhances human thyroid carcinoma cell invasion through urokinase activity. *Int J Biochem Cell Biol.* 2008;40(9):1890-1900. doi:10.1016/j.biocel.2008.01.023
21. Tong Y, Sun P, Yong J, et al. Radiogenomic analysis of papillary thyroid carcinoma for prediction of cervical lymph node metastasis: a preliminary study. *Front Oncol.* 2021;11(/):682998. doi:10.3389/fonc.2021.682998
22. Ghoneim C, Soula-Rothhut M, Rothhut B. Thrombospondin-1 in differentiated thyroid cancer: Dr. Jekyll and Mr. Hyde. *Connect Tissue Res.* 2008;49(3):257-260. doi:10.1080/03008200802147795
23. Zhang X, Huang T, Li Y, Qiu H. Upregulation of THBS1 is related to immunity and chemotherapy resistance in gastric cancer. *Int J Gen Med.* 2021;14(/):4945-4957. doi:10.2147/ijgm.S329208
24. von Elm E, Altman DG, Egger M, Pocock SJ, Gøtzsche PC, Vandenbroucke JP. The strengthening the reporting of observational studies in epidemiology (STROBE) statement: guidelines for reporting observational studies. *Ann Intern Med.* 2007;147(8):573-577. doi:10.7326/0003-4819-147-8-200710160-00010
25. Haugen BR, Alexander EK, Bible KC, et al. 2015 American thyroid association management guidelines for adult patients with thyroid nodules and differentiated thyroid cancer: the American thyroid association guidelines task force on thyroid nodules and differentiated thyroid cancer. *Thyroid.* 2016;26(1):1-133. doi:10.1089/thy.2015.0020
26. Chen Y, Li ZY, Zhou GQ, Sun Y. An immune-related gene prognostic index for head and neck squamous cell carcinoma. *Clin Cancer Res: Off J Am Assoc Cancer Res.* 2021;27(1):330-341. doi:10.1158/1078-0432.Ccr-20-2166
27. Tang J, Kong D, Cui Q, et al. Prognostic genes of breast cancer identified by gene co-expression network analysis. *Front Oncol.* 2018;8(/):374. doi:10.3389/fonc.2018.00374
28. Fu J, Li K, Zhang W, et al. Large-scale public data reuse to model immunotherapy response and resistance. *Genome Med.* 2020;12(1):21. doi:10.1186/s13073-020-0721-z
29. Jiang P, Gu S, Pan D, et al. Signatures of T cell dysfunction and exclusion predict cancer immunotherapy response. *Nat Med.* 2018;24(10):1550-1558. doi:10.1038/s41591-018-0136-1
30. Li B, Severson E, Pignon JC, et al. Comprehensive analyses of tumor immunity: implications for cancer immunotherapy. *Genome Biol.* 2016;17(1):174. doi:10.1186/s13059-016-1028-7
31. Li T, Fan J, Wang B, et al. TIMER: a Web server for comprehensive analysis of tumor-infiltrating immune cells. *Cancer Res.* 2017;77(21):e108-e110. doi:10.1158/0008-5472.Can-17-0307
32. Li T, Fu J, Zeng Z, et al. TIMER2.0 for analysis of tumor-infiltrating immune cells. *Nucleic Acids Res.* 2020;48(W1):W509-w514. doi:10.1093/nar/gkaa407
33. Nucera C, Porrello A, Antonello ZA. B-Raf(V600E) and thrombospondin-1 promote thyroid cancer progression. *Proc Natl Acad Sci U S A.* 2010;107(23):10649-10654. doi:10.1073/pnas.1004934107
34. Tanaka K, Sonoo H, Kurebayashi J, et al. Inhibition of infiltration and angiogenesis by thrombospondin-1 in papillary thyroid carcinoma. *Clin Cancer Res: Off J Am Assoc Cancer Res.* 2002;8(5):1123-1131.
35. Prete A, Lo AS, Sadow PM, et al. Pericytes elicit resistance to vemurafenib and sorafenib therapy in thyroid carcinoma via the TSP-1/TGFβ1 axis. *Clin Cancer Res: Off J Am Assoc Cancer Res.* 2018;24(23):6078-6097. doi:10.1158/1078-0432.Ccr-18-0693
36. Nikiforov YE, Nikiforova MN. Molecular genetics and diagnosis of thyroid cancer. *Nat Rev Endocrinol.* 2011;7(10):569-580. doi:10.1038/nrendo.2011.142
37. Wu Q, Jiang L, Wu J, Dong H, Zhao Y. Klotho inhibits proliferation in a RET fusion model of papillary thyroid cancer by regulating the Wnt/β-catenin pathway. *Cancer Manag Res.* 2021;13(/):4791-4802. doi:10.2147/cmar.S295086
38. Lv P, Xue Y. ETS like-1 protein ELK1-induced lncRNA LINC01638 accelerates the progression of papillary thyroid cancer by regulating Axin2 through Wnt/β-catenin signaling pathway. *Bioengineered.* 2021;12(1):3873-3885. doi:10.1080/21655979.2021.1935404
39. Park JY, Yi JW, Park CH, et al. Role of BRAF and RAS mutations in extrathyroidal extension in papillary thyroid cancer. *Cancer Genom Proteom.* 2016;13(2):171-181.
40. Gong J, Jin B, Shang L, Liu N. Characterization of the immune cell infiltration landscape of thyroid cancer for improved immunotherapy. *Front Mol Biosci.* 2021;8(/):714053. doi:10.3389/fmolb.2021.714053
41. Ferrari SM, Fallahi P, Galdiero MR, et al. Immune and inflammatory cells in thyroid cancer microenvironment. *Int J Mol Sci.* 2019;20(18):4413. doi:10.3390/ijms20184413
42. Zhi J, Zhang P, Zhang W, et al. Inhibition of BRAF sensitizes thyroid carcinoma to immunotherapy by enhancing tsMHCII-mediated immune recognition. *J Clin Endocrinol Metab.* 2021;106(1):91-107. doi:10.1210/clinem/dgaa656
43. Stenman A, Backman S, Johansson K, et al. Pan-genomic characterization of high-risk pediatric papillary thyroid carcinoma. *Endocr Relat Cancer.* 2021;28(5):337-351. doi:10.1530/erc-20-0464
44. Zheng L, Li S, Zheng X, Guo R, Qu W. AHNAK2 Is a novel prognostic marker and correlates with immune infiltration in papillary thyroid cancer: evidence from integrated analysis. *Int Immunopharmacol.* 2021;90(/):107185. doi:10.1016/j.intimp.2020.107185
45. Xiao M, Zhang J, Chen W, Chen W. M1-like tumor-associated macrophages activated by exosome-transferred THBS1 promote malignant migration in oral squamous cell carcinoma. *J Exp Clin Cancer Res.* 2018;37(1):143. doi:10.1186/s13046-018-0815-2
46. Chao CC, Lee WF, Wang SW, et al. CXC Chemokine ligand-13 promotes metastasis via CXCR5-dependent signaling pathway in non-small cell lung cancer. *J Cell Mol Med.* 2021;90(/):107185. doi:10.1111/jcmm.16743
47. Sun X, Chen Q, Zhang L, Chen J, Zhang X. Exploration of prognostic biomarkers and therapeutic targets in the microenvironment of bladder cancer based on CXC chemokines. *Math Biosci Eng: MBE.* 2021;18(5):6262-6287. doi:10.3934/mbe.2021313
48. Qian G, Wu M, Zhao Y, et al. Thyroid cancer metastasis is associated with an overabundance of defective follicular helper T cells. *APMIS: Acta Pathol Microbiol Immunol Scand.* 2020;128(8):487-496. doi:10.1111/apm.13062
49. Jain N, Thompson P, Burger J, et al. Ibrutinib, fludarabine, cyclophosphamide, and obinutuzumab (iFCG) regimen for chronic lymphocytic leukemia (CLL) with mutated IGHV and without TP53 aberrations. *Leukemia.* 2021;35(12):3421-3429. doi:10.1038/s41375-021-01280-8

50. Wang Y, Liu Y, Chen L, et al. T cell receptor Beta-chain profiling of tumor tissue, peripheral blood and regional lymph nodes from patients with papillary thyroid carcinoma. *Front Immunol.* 2021;12():595355. doi:10.3389/fimmu.2021.595355
51. Caronia LM, Phay JE, Shah MH. Role of BRAF in thyroid oncogenesis. *Clin Cancer Res: Off J Am Assoc Cancer Res.* 2011;17(24):7511-7517. doi:10.1158/1078-0432.Ccr-11-1155
52. Guo TA, Wu YC, Tan C, et al. Clinicopathologic features and prognostic value of KRAS, NRAS and BRAF mutations and DNA mismatch repair status: a single-center retrospective study of 1,834 Chinese patients with stage I-IV colorectal cancer. *Int J Cancer.* 2019;145(6):1625-1634. doi:10.1002/ijc.32489